Clinical and Experimental Obstetrics & Gynecology

Clin. Exp. Obstet. Gynecol. **2026**; 53(3): 45628
https://doi.org/10.31083/CEOG45628

Original Research

Application of a Nomogram Integrating Ultrasound Data With Clinical Characteristics to Differentiate Between Uterine Sarcoma and Uterine Fibroids

Chunzhen Huang[1,*,†], Yujuan Weng[2,†], Baiwei Lin[2]

[1]Department of Ultrasound, Affiliated Hospital of Putian University & Putian Children's Hospital, 351100 Putian, Fujian, China
[2]Department of Ultrasound, Affiliated Hospital of Putian University, 351100 Putian, Fujian, China
*Correspondence: hczyeah@163.com (Chunzhen Huang)
[†]These authors contributed equally.

Academic Editors: Ugo Indraccolo and Michael H. Dahan
Submitted: 8 August 2025 Revised: 6 November 2025 Accepted: 12 December 2025 Published: 16 March 2026

Abstract

Background: To assess the diagnostic value of a nomogram that integrates ultrasound and clinical features to differentiate uterine sarcoma from uterine fibroids. **Methods**: In this retrospective analysis, data from 60 uterine sarcoma patients and 60 uterine fibroid patients confirmed by surgical pathology at the Affiliated Hospital of Putian University (August 2024–June 2025) were examined. Clinical variables (age, disease duration, menopausal status, postmenopausal bleeding), laboratory markers (carbohydrate antigen 125 [CA125], lactate dehydrogenase [LDH]), and ultrasound characteristics (maximal diameter, margin, echogenicity, cystic change, calcification, and Adler blood flow grading) were collected. Independent predictors were determined through both univariate and multivariate logistic regression analyses. Predictive models were constructed and evaluated via receiver operating characteristic (ROC) curves, with model robustness further assessed through tenfold cross-validation and bootstrap validation. **Results**: The groups were successfully matched for key baseline characteristics (age, disease duration, menopausal status; all $p > 0.05$). Multivariate analysis revealed that age, postmenopausal bleeding, LDH, CA125, echogenicity, and tumor margin were independent predictors. The combined model demonstrated enhanced diagnostic ability with an area under the curve (AUC) of 0.902 (95% CI: 0.847–0.935), outperforming individual models based on clinical (AUC: 0.764), laboratory (AUC: 0.651), and ultrasound (AUC: 0.804) data. The model's generalizability was confirmed by internal validation, showing strong maintained performance (tenfold cross-validated AUC: 0.885; bootstrap-corrected AUC: 0.887). **Conclusion**: A nomogram based on combined clinical, laboratory, and ultrasound features provides high accuracy for differentiating uterine sarcoma from fibroids, supporting clinical decision-making.

Keywords: uterine sarcoma; uterine fibroids; nomogram; ultrasound; differential diagnosis

1. Introduction

Uterine sarcoma is a rare but highly aggressive malignancy of the female reproductive tract that accounts for a small proportion of uterine tumors but has a poor prognosis due to its rapid progression and early metastasis [1–3]. In contrast, uterine fibroids (leiomyomas) are benign smooth muscle tumors and represent the predominant gynecological tumors found among women of childbearing age [4,5]. Despite considerable differences in therapeutic strategies and prognoses, differentiating uterine sarcoma from fibroids remains a significant clinical challenge, especially in the preoperative setting [6,7]. Previous research have identified several sonographic features that may aid in distinguishing uterine sarcomas from fibroids [1,6,7]. A comprehensive meta-analysis systematically reviewed ultrasound characteristics that could differentiate these tumors [8]. The key distinguishing features include (1) irregular tumor margins, (2) heterogeneous internal echogenicity, (3) the presence of cystic degeneration, (4) increased vascularity with high Doppler flow indices, and (5) the presence of necrotic or hemorrhagic areas. However, no single ultrasound feature provides a definitive diagnosis, highlighting the need for a comprehensive approach. Conventional imaging modalities such as ultrasound can offer valuable information regarding tumor morphology, vascularity, and internal characteristics. However, the similarity of imaging characteristics shared by benign and malignant uterine tumors often leads to misdiagnosis [9,10]. The integration of multidimensional data encompassing clinical factors, laboratory markers, and advanced ultrasound parameters may improve diagnostic accuracy and aid clinicians in personalized decision-making [11].

Nomogram models are widely used in oncology for risk stratification, prediction, and individualized assessment by converting complex statistical predictions into intuitive visual tools [12–14]. To date, few studies have systematically evaluated the performance of nomograms incorporating both ultrasound and clinical features in distinguishing between uterine sarcoma and fibroids.

Accordingly, this research seeks to establish and verify a nomogram incorporating clinical, laboratory, and ultrasound characteristics to improve presurgical discrimina-

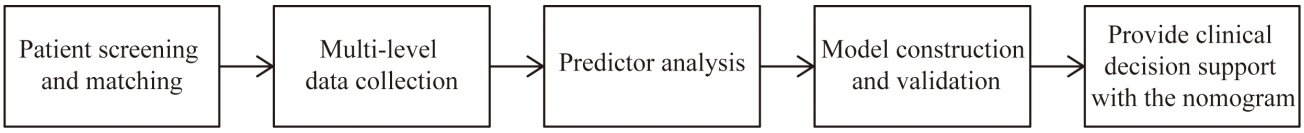

Fig. 1. Flowchart of this study.

tion between uterine sarcoma and fibroids, thus facilitating timely and appropriate clinical management.

2. Materials and Methods

2.1 Study Design and Patients

The overall research process, including patient screening, data collection, and model validation, is illustrated in Fig. 1. This study retrospectively reviewed the clinical records collected at the Affiliated Hospital of Putian University from August 2024 to June 2025. Sixty individuals diagnosed with uterine sarcoma and another 60 with uterine fibroids, all confirmed by pathological examination, were included. The inclusion criteria were as follows: (1) had a diagnosis of uterine sarcoma or fibroid confirmed by surgical pathology; (2) all patients underwent color Doppler ultrasound for subsequent analysis; (3) complete clinical and laboratory data were available for all patients to ensure the accuracy and reliability of the study; and (4) patients in all age groups, including both premenopausal and postmenopausal women, were included. The exclusion criteria were as follows: (1) patients with concomitant malignancies, which could interfere with the diagnosis and analysis of uterine sarcoma or fibroids; (2) long-term estrogen use, as estrogen may influence tumor development and cause bias; (3) patients diagnosed with nonprimary uterine sarcoma to ensure the specificity and consistency of the study cohort; and (4) patients who did not undergo ultrasound examination or who had significant missing clinical or laboratory data to ensure data validity and scientific rigor. The diagnoses of all the patients were independently assessed by two senior pathologists in a blinded manner and confirmed according to the 2020 World Health Organization (WHO) classification of female genital tumors [15]. For the identification of sarcomatoid changes, the following morphological criteria were strictly followed: (1) prominent nuclear atypia (increased nuclear-cytoplasmic ratio, mitotic count $\geq$10/10 high-power fields [HPF]); (2) tumor cells arranged in a spindle or epithelioid pattern with disarray; (3) presence of pathological mitoses; and (4) associated with tumor necrosis. In cases of diagnostic disagreement between the two pathologists, a third senior pathologist was consulted to make the final decision.

2.2 Collection of Clinical Data and Ultrasound Parameters

This retrospective, single-center case-control study followed the STROBE guidelines and employed a 1:1 matched design to minimize selection bias, carefully matching 60 uterine sarcoma patients and 60 uterine fibroid patients based on age ($\pm$3 years), menopausal status, and disease duration ($\pm$1 year). The primary outcome was the diagnostic performance of a nomogram integrating clinical, laboratory, and ultrasound features in differentiating uterine sarcoma from fibroids, with key endpoints including diagnostic accuracy, sensitivity, specificity, and area under the receiver operating characteristic (ROC) curve (AUC). Matching was performed by an independent researcher blinded to the final diagnosis, and a standardized data collection protocol was implemented to ensure comprehensive and consistent data acquisition across all participants. The analysis of the ultrasound images was independently completed by 2 experienced sonographers. All ultrasound features were evaluated according to the standardized terminology and definitions published by the International Endometrial Tumor Analysis (IETA) [16]. For key parameters such as tumor margins, internal echoes, and blood flow distribution, the classification criteria in the Morphological Uterine Sonographic Assessment (MUSA) consensus were adopted to ensure the consistency and accuracy of the terminology used. For the radiological identification of sarcomatoid changes, the following criteria were used: irregular margins (defined as ill-defined or infiltrative growth), highly heterogeneous internal echoes (defined as a difference in echo intensity $>$50%), and an Adler blood flow grade $\geq$3 (characterized by diffuse vascular distribution with a resistance index [RI] $<$0.4). A consensus was reached through discussion for all controversial cases.

2.3 Model Construction

The data were categorized into three groups, namely, clinical information, laboratory indicators, and ultrasound features, and analyzed via Python (version 3.12.3; Python Software Foundation, Beaverton, OR, USA). Independent predictors in each group were identified through univariate and multivariate analyses. Four predictive models were constructed: clinical, laboratory, ultrasound, and combined models. The diagnostic performance of each model was assessed via ROC curves to determine the AUC, sensitivity, and specificity. The DeLong test was used to compare the predictive ability of the models. To rigorously evaluate the models' generalizability and mitigate overfitting, we employed two internal validation techniques. First, tenfold cross-validation was performed by randomly partitioning the dataset into 10 equal-sized folds. The models were trained on 9 folds and validated on the remaining fold; this process was repeated 10 times, and the performance met-

Table 1. Baseline characteristics of the study participants.

Characteristic	Uterine fibroids (n = 60)	Uterine sarcoma (n = 60)	*p* value
Demographic & clinical			
Age (years), mean ± SD	48.52 ± 5.73	50.10 ± 4.84	0.105
Disease duration (years), mean ± SD	5.83 ± 0.62	5.63 ± 0.65	0.087
Menopausal status, n (%)			0.754
Premenopausal	38 (63.3%)	36 (60.0%)	
Postmenopausal	22 (36.7%)	24 (40.0%)	
Postmenopausal bleeding, n (%)	4 (6.7%)	18 (30.0%)	0.002
Laboratory markers			
LDH (U/L), median (IQR)	185.5 (162–210)	245.0 (218–285)	<0.001
CA125 (U/mL), median (IQR)	28.0 (20–40)	65.5 (45–92)	<0.001
Ultrasound features			
Maximal diameter (cm), mean ± SD	6.5 ± 2.1	7.8 ± 3.2	0.010
Margin, n (%)			<0.001
Regular	52 (86.7%)	20 (33.3%)	
Irregular	8 (13.3%)	40 (66.7%)	
Echogenicity, n (%)			0.003
Homogeneous	45 (75.0%)	28 (46.7%)	
Heterogeneous	15 (25.0%)	32 (53.3%)	
Cystic change, n (%)	10 (16.7%)	26 (43.3%)	0.003
Calcification, n (%)	12 (20.0%)	8 (13.3%)	0.462
Adler blood flow grade, n (%)			<0.001
Grade 1–2	48 (80.0%)	22 (36.7%)	
Grade 3–4	12 (20.0%)	38 (63.3%)	

LDH, lactate dehydrogenase; CA125, carbohydrate antigen 125; IQR, interquartile range.

rics were averaged to yield a robust estimate. Second, bootstrap validation with 1000 repetitions was conducted. For each repetition, a bootstrap sample of the same size as the original dataset was drawn with replacement to train the model, which was then evaluated on the original dataset. The optimism (i.e., the difference between the bootstrap performance and the apparent performance) was calculated for each repetition and averaged to obtain an optimism-corrected estimate of the models' performance.

2.4 Statistical Analysis

All the statistical calculations were conducted via Python (version 3.12.3; Python Software Foundation, Beaverton, OR, USA) and IBM SPSS Statistics (v 26.0; IBM Corp., Armonk, NY, USA). The kappa test was used to assess the diagnostic consistency among pathologists (Kappa = 0.82, $p < 0.001$) and the evaluation consistency among sonographers (Kappa = 0.76, $p < 0.001$), indicating a high level of consistency. Continuous variables exhibiting a normal distribution are presented as the mean ± standard deviation, whereas those not following a normal distribution are presented as the median and interquartile range. The chi-square test was applied to compare categorical data. For the three feature groups, both univariate and multivariate regression analyses were utilized. Statistical results with *p* values less than 0.05 were interpreted as significant.

3. Results

3.1 Comparison of Baseline Characteristics

The baseline characteristics of the study participants are summarized in Table 1. Successful matching was confirmed for age, disease duration, and menopausal status, as no significant differences were observed between the two groups (all $p > 0.05$). However, significant differences were found in postmenopausal bleeding ($p = 0.002$), laboratory markers including lactate dehydrogenase (LDH) ($p < 0.001$) and carbohydrate antigen 125 (CA125) ($p < 0.001$), and ultrasound features such as maximal diameter ($p = 0.010$), margin ($p < 0.001$), echogenicity ($p = 0.003$), cystic change ($p = 0.003$), and Adler blood flow grade ($p < 0.001$). Calcification did not differ significantly between the groups ($p = 0.462$).

3.2 Univariate Regression Analysis

Univariate logistic regression analysis indicated that age (OR = 2.105, $p = 0.002$), menopausal status (OR = 5.222, $p < 0.001$), and postmenopausal vaginal bleeding (OR = 14.03, $p = 0.003$) were significantly associated with sarcoma risk. Laboratory indices such as LDH (OR = 2.189, $p < 0.001$) and CA125 (OR = 2.592, $p < 0.001$) were also identified as significant predictors. Among the ultrasound features, echogenicity (OR = 0.415, $p = 0.011$), margin (OR = 7.094, $p < 0.001$), sarcomatoid changes (OR = 4.239, $p = 0.001$), and maximal tumor diameter (OR = 1.246, $p = 0.030$) had a significant diagnostic impact (Table 2, Fig. 2).

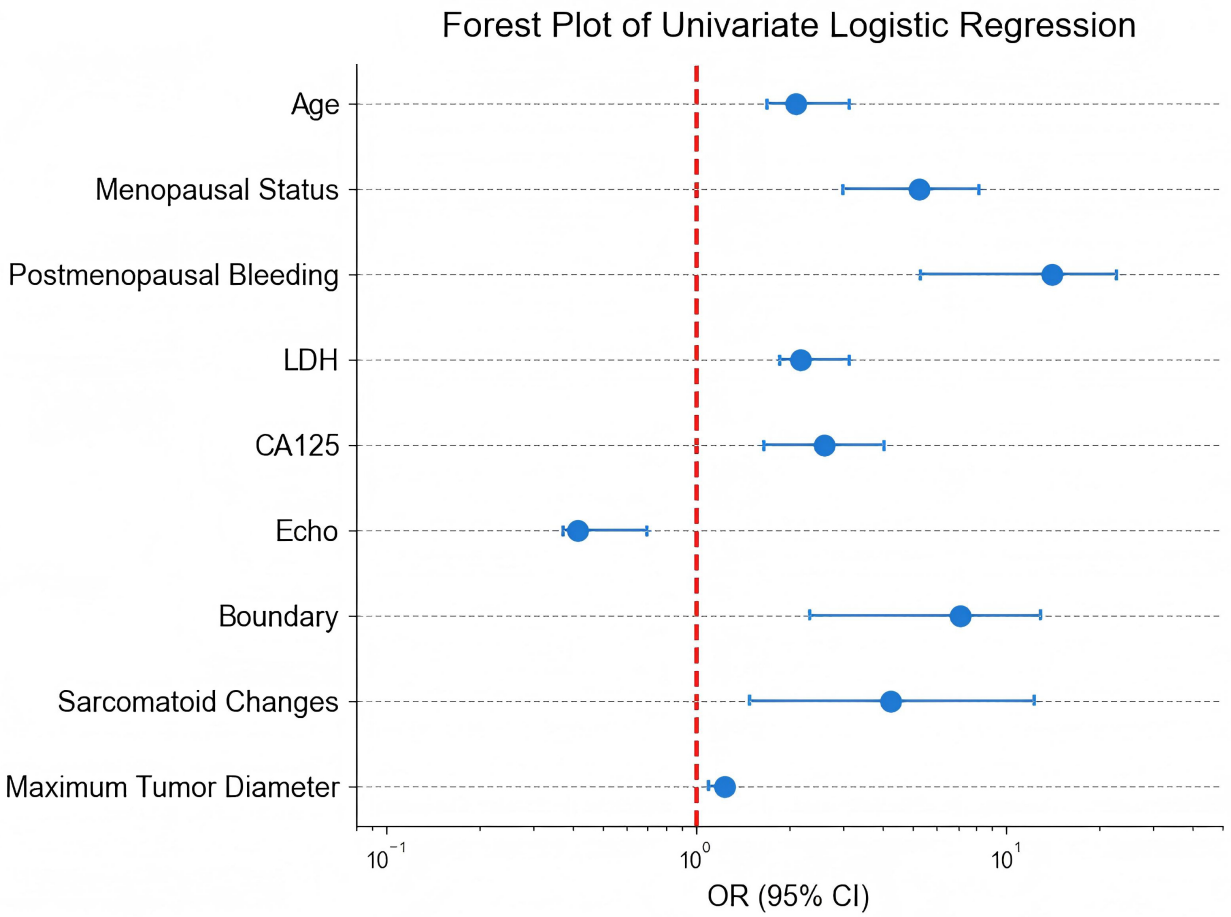

Fig. 2. Forest plot of the univariate logistic regression analysis. OR, odds ratio; CI, confidence interval; LDH, lactate dehydrogenase; CA125, carbohydrate antigen 125.

Table 2. Univariate logistic regression analysis of clinical characteristics between patients with uterine sarcoma and those with uterine fibroids.

Feature	OR	95% CI	*p* value
Age	2.105	1.700–3.140	0.002
Menopausal status	5.222	3.000–8.200	<0.001
Postmenopausal bleeding	14.030	5.308–22.843	0.003
LDH	2.189	1.874–3.141	<0.001
CA125	2.592	1.652–4.071	<0.001
Echo	0.415	0.372–0.700	0.011
Margin	7.094	2.331–13.007	<0.001
Sarcomatoid changes	4.239	1.503–12.343	0.001
Maximum tumor diameter	1.246	1.100–1.300	0.030

3.3 Multivariate Regression Analysis

The outcomes from the multivariate logistic regression analysis are presented in Table 3 and Fig. 3. Multiple factors, including age (OR = 1.805, 95% CI: 1.225–3.749, $p < 0.001$) and postmenopausal vaginal bleeding (OR = 8.182, 95% CI: 4.508–15.045, $p = 0.002$), were confirmed as independent predictors for sarcoma. In contrast, menopausal status was not an independent predictor in the multivariate model (OR = 0.565, 95% CI: 0.256–1.217, $p = 0.802$). Laboratory markers LDH (OR = 1.316, 95% CI: 1.107–1.606, $p = 0.007$) and CA125 (OR = 1.816, 95% CI: 1.153–2.394, $p = 0.002$) remained significant predictors. Among the ultrasound features, echogenicity (OR = 0.481, $p = 0.003$) and margin (OR = 6.514, $p < 0.001$) were independently associated. In contrast, tumor morphology (OR = 1.015, $p = 0.211$) and maximal diameter (OR = 1.414, $p = 0.574$) were not significant in the multivariate analysis.

3.4 Model Evaluation

The diagnostic performance of various models is presented in Table 4 and Fig. 4. The apparent performance on the original dataset showed that the clinical model yielded an AUC of 0.764, indicating good discriminative ability; the laboratory model reached an AUC of 0.651; and the ultrasound model exhibited a higher AUC of 0.804. Importantly, the integrated clinical-laboratory-USA model achieved the highest AUC of 0.902, significantly outperforming all single models (all DeLong $p < 0.05$).

To rigorously assess the models' generalizability and correct for overoptimism, internal validation was per-

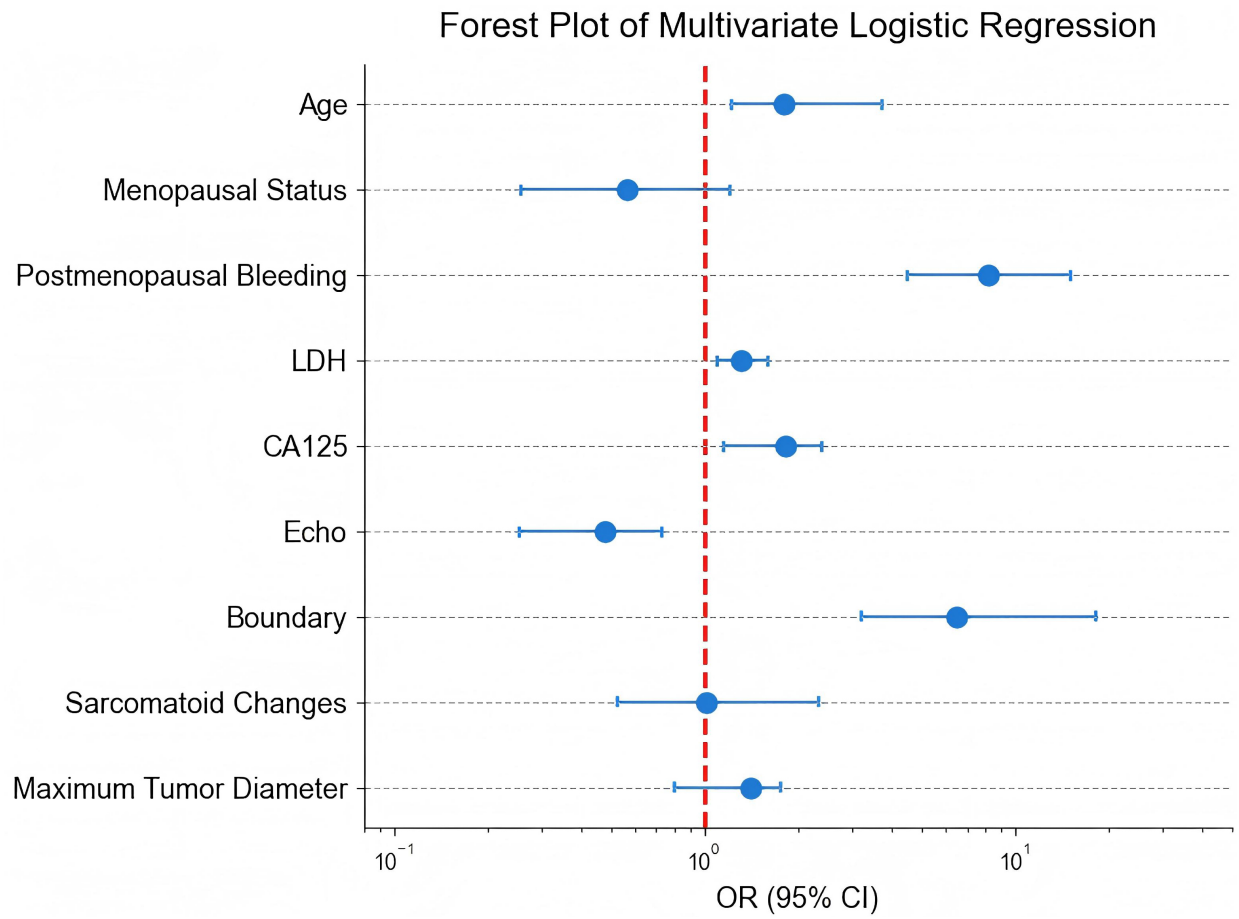

Fig. 3. Forest plot of multivariate logistic regression analysis.

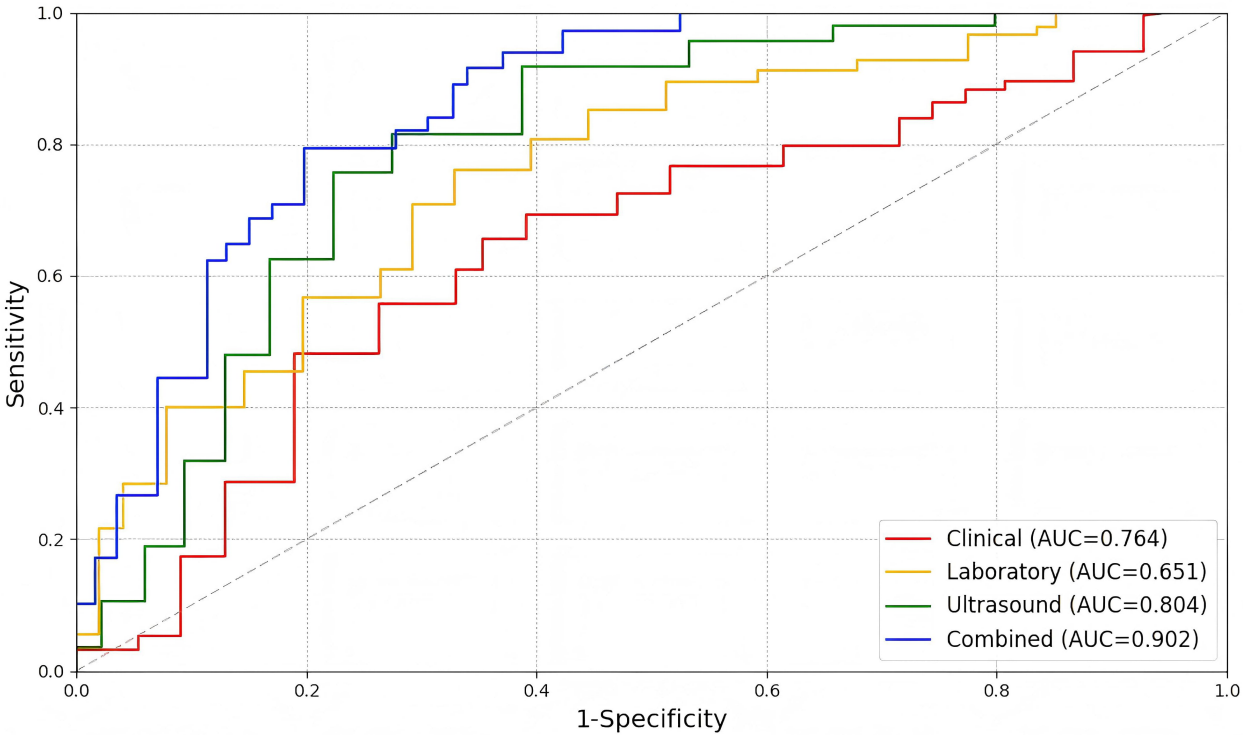

Fig. 4. Predictive performance of the four models. AUC, area under the curve.

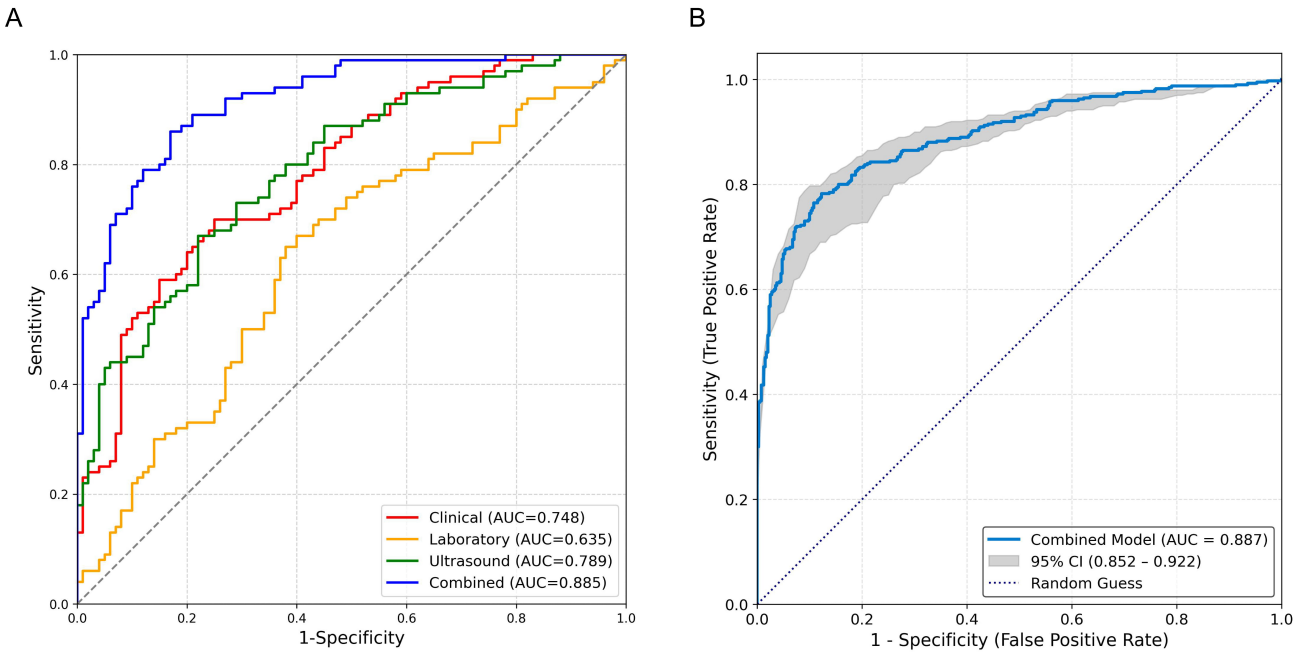

Fig. 5. Predictive performance and internal validation of the models. (A) ROC curves from tenfold cross-validation. The lines represent the mean ROC curve for each model averaged over the 10 folds. The combined model (AUC = 0.885) demonstrates superior discriminative ability compared to the clinical (AUC = 0.748), laboratory (AUC = 0.635), and ultrasound (AUC = 0.789) models. (B) Bootstrap-validated ROC curve of the combined model. The solid line represents the optimism-corrected mean ROC curve from 1000 bootstrap repetitions (AUC = 0.887). The shaded area represents the 95% confidence interval, illustrating the model's stable performance. ROC, receiver operating characteristic; AUC, area under the curve.

Table 3. Multivariate logistic regression analysis of clinical characteristics between patients with uterine sarcoma and those with uterine fibroids.

Feature	OR	95% CI	*p* value
Age	1.805	1.225–3.749	<0.001
Menopausal status	0.565	0.256–1.217	0.802
Postmenopausal bleeding	8.182	4.508–15.045	0.002
LDH	1.316	1.107–1.606	0.007
CA125	1.816	1.153–2.394	0.002
Echo	0.481	0.253–0.728	0.003
Margin	6.514	3.199–18.135	<0.001
Sarcomatoid changes	1.015	0.524–2.329	0.211
Maximum tumor diameter	1.414	0.803–1.761	0.574

formed (Fig. 5). The tenfold cross-validated AUCs for the clinical, laboratory, ultrasound, and combined models were 0.748, 0.635, 0.789, and 0.885, respectively. Furthermore, bootstrap validation with 1000 repetitions yielded optimism-corrected AUCs of 0.751, 0.640, 0.791, and 0.887 for the respective models. The combined model maintained the highest performance across all validation methods, demonstrating its robust diagnostic ability.

4. Discussion

In this study, we developed and validated a nomogram that integrates readily accessible clinical, laboratory, and ultrasound features to preoperatively differentiate uterine sarcoma from fibroids. Our key findings from multivariate analysis identified age, postmenopausal bleeding, elevated LDH and CA125 levels, along with heterogeneous echogenicity and irregular tumor margins on ultrasound as independent predictors of uterine sarcoma. The core innovation of our research lies in the integration of these multidimensional parameters into a single, accessible tool.

The superior performance of our combined model, achieving an apparent AUC of 0.902, underscores the synergistic value of integrating data from different sources. This integrated approach significantly outperformed models based on clinical, laboratory, or ultrasound features alone, which is consistent with the complex nature of the disease and suggests that a single-modality assessment is insufficient for optimal discrimination. Crucially, the model's robustness and generalizability were confirmed through rigorous internal validation. The combined model maintained high performance with a tenfold cross-validated AUC of 0.885 and a bootstrap-corrected AUC of 0.887. The narrow confidence intervals around these validated estimates provide strong evidence that the model is stable and not substantially overfitted, thereby addressing a key concern in predictive model development and enhancing its potential credibility for clinical application.

We explicitly acknowledge that magnetic resonance imaging (MRI) is a highly sensitive imaging modality for

Table 4. Comparison of predictive performance among different models.

Performance metric	Clinical model	Laboratory model	Ultrasound model	Combined model
Sensitivity, % (95% CI)	84.5 (74.2–91.3)	68.3 (57.5–79.1)	70.4 (66.2–78.5)	90.8 (83.2–94.4)
Specificity, % (95% CI)	60.3 (51.8–71.3)	65.1 (55.2–73.6)	83.1 (75.7–90.1)	85.8 (76.8–94.8)
Accuracy, % (95% CI)	76.2 (67.5–84.9)	66.5 (58.4–74.7)	77.1 (69.4–83.9)	88.3 (82.0–94.1)
p value	0.005	0.013	0.002	0.001
AUC (Apparent), (95% CI)	0.764 (0.702–0.863)	0.651 (0.568–0.733)	0.804 (0.736–0.872)	0.902 (0.847–0.935)
AUC (10-fold CV), (95% CI)	0.748 (0.698–0.798)	0.635 (0.575–0.695)	0.789 (0.739–0.839)	0.885 (0.845–0.925)
AUC (Bootstrap), (95% CI)	0.751 (0.705–0.797)	0.640 (0.590–0.690)	0.791 (0.741–0.841)	0.887 (0.852–0.922)

AUC, area under the curve; CV, cross-validation.

soft tissue characterization. However, our nomogram deliberately excludes MRI data for multidimensional reasons aimed at highlighting the practicality and broad applicability of the study, as detailed below.

4.1 Focus on Developing an Accessible Screening Tool

The core objective of this study is to construct a cost-effective, easily implementable preoperative triage tool for resource-limited settings. Although MRI is highly sensitive, it has significant limitations in primary care scenarios, including high costs, poor equipment availability, and lengthy examination times. In contrast, our nomogram integrates clinical features, laboratory markers, and ultrasound parameters to provide a rapid and economical first-line screening method. This approach aims to identify high-risk patients who can then be referred for more precise MRI evaluation.

4.2 Consistency With Existing Literature Strategies

Our approach aligns with recent literature advocating the need for efficient preliminary diagnostic tools [17–20]. For example, in resource-constrained areas, the low availability of MRI can lead to diagnostic delays. The nomogram, as a multidimensional integration model, can prioritize high-risk cases and optimize the allocation of medical resources. This stepwise strategy (initial screening with the nomogram followed by MRI confirmation) has been proven to enhance diagnostic efficiency and reduce unnecessary invasive procedures. This stepwise diagnostic strategy, initial risk stratification with the nomogram followed by targeted MRI confirmation in high-risk cases has the potential to enhance overall diagnostic efficiency, reduce unnecessary invasive procedures, and ensure timely referral for complex cases.

4.3 Enhancing Clinical Feasibility

By avoiding direct reliance on MRI, our model lowers the barriers to clinical implementation. Ultrasound and clinical data are more readily accessible and easier to implement in primary healthcare settings, which aligns with the global health equity concept. Future multicenter studies can further validate the complementary value of this model when it is used in conjunction with MRI.

In summary, the exclusion of MRI is based on a comprehensive consideration of practicality, cost-effectiveness, and accessibility. Our nomogram aims to bridge the gap between primary screening and advanced imaging, providing efficient support for clinical decision-making.

Comparing our study with the literature, we observed significant parallels and distinctions [21,22]. One study developed a similar diagnostic model with an AUC of 0.82, which is comparable to our integrated model's performance (AUC = 0.902) [23]. Our research extends this approach by integrating ultrasound characteristics, demonstrating improved diagnostic accuracy [24–26]. Our research extends this approach not only by integrating ultrasound characteristics but also by subjecting the model to more rigorous validation, thereby providing a more reliable estimate of its future performance. Unlike previous studies that relied primarily on single-modality assessments, our nomogram's strength lies in its multidimensional data integration, which significantly enhances diagnostic precision. These comparisons underscore the innovative nature of our approach and its potential clinical utility in differentiating uterine sarcomas from fibroids.

4.4 Limitations

Despite these promising results, this study has several limitations that should be acknowledged. First, its retrospective and single-center design may introduce selection bias and limit the generalizability of our findings. Although we employed a 1:1 matched design to mitigate this risk, future prospective, multicenter studies with larger sample sizes are warranted to validate and refine our nomogram.

Second, the relatively small sample size, particularly for rare uterine sarcoma cases, may affect the stability and statistical power of the predictive model. Expanding the cohort in future research would help enhance the model's robustness.

Third, while the nomogram demonstrates high diagnostic accuracy, it is intended as a preoperative triage tool rather than a replacement for definitive diagnostic methods such as MRI or histopathological examination. Its performance in routine clinical practice needs further evaluation.

5. Conclusion

In summary, our study demonstrates that integrating clinical, laboratory, and ultrasound features substantially improves the diagnostic accuracy for differentiating uterine sarcoma from fibroids. The combined predictive model holds significant potential for improving clinical decision-making and patient prognosis.

Availability of Data and Materials

The experimental data used to support the findings of this study are available from the corresponding author upon request.

Author Contributions

CZH contributed to the study conception and drafted the manuscript; YJW performed the data analysis; BWL designed the research project and collected the data. All authors have read and approved the final manuscript. All authors contributed to editorial changes in the manuscript. All authors have participated sufficiently in the work and agreed to be accountable for all aspects of the work.

Ethics Approval and Consent to Participate

This study was conducted in accordance with the guidelines of the Declaration of Helsinki, and the research protocol has been approved by the Ethics Committee of the Affiliated Hospital of Putian University (Ethical approval number: 2025282). All patients provided informed consent before participating in the study.

Acknowledgment

Not applicable.

Funding

This research received no external funding.

Conflict of Interest

The authors declare no conflict of interest.

Declaration of AI and AI-Assisted Technologies in the Writing Process

During the preparation of this work the authors used ChatGpt-3.5 in order to check spell and grammar. After using this tool, the authors reviewed and edited the content as needed and takes full responsibility for the content of the publication.

Supplementary Material

Supplementary material associated with this article can be found, in the online version, at https://doi.org/10.31083/CEOG45628.

References

[1] Ciccarone F, Biscione A, Robba E, Pasciuto T, Giannarelli D, Gui B, *et al*. A clinical ultrasound algorithm to identify uterine sarcoma and smooth muscle tumors of uncertain malignant potential in patients with myometrial lesions: the MYometrial Lesion UltrasouNd And mRi study. American Journal of Obstetrics and Gynecology. 2025; 232: 108.e1–108.e22. https://doi.org/10.1016/j.ajog.2024.07.027.

[2] Alloush K, El Hamamy S, Peevor R, Oosterhouse T. Uterine Leiomyosarcoma Diagnosed at Caesarean Myomectomy: A Case Report. Cureus. 2025; 17: e96468. https://doi.org/10.7759/cureus.96468.

[3] Lebar V, Čelebić A, Calleja-Agius J, Jakimovska Stefanovska M, Drusany Staric K. Advancements in uterine sarcoma management: A review. European Journal of Surgical Oncology: the Journal of the European Society of Surgical Oncology and the British Association of Surgical Oncology. 2025; 51: 109646. https://doi.org/10.1016/j.ejso.2025.109646.

[4] Goad J, Rajkovic A. Uterine fibroids at single-cell resolution: unveiling cellular heterogeneity to improve understanding of pathogenesis and guide future therapies. American Journal of Obstetrics and Gynecology. 2025; 232: S124–S134. https://doi.org/10.1016/j.ajog.2024.08.037.

[5] de Smit NS, de Lange ME, Boomsma MF, Huirne JAF, Hehenkamp WJK. Current treatment for symptomatic uterine fibroids: available evidence and therapeutic dilemmas. Lancet (London, England). 2025; 406: 91–102. https://doi.org/10.1016/S0140-6736(25)00728-7.

[6] Kim J, Williams A, Noh H, Jasper EA, Jones SH, Jaworski JA, *et al*. Genome-wide meta-analysis identifies novel risk loci for uterine fibroids within and across multiple ancestry groups. Nature Communications. 2025; 16: 2273. https://doi.org/10.1038/s41467-025-57483-5.

[7] Yamanishi Y, Kotani Y, Kido A, Otani T, Himoto Y, Kurata Y, *et al*. Differentiation of uterine fibroids and sarcomas by MRI and serum LDH levels: a multicenter study of the KAMOGAWA study. Journal of Gynecologic Oncology. 2025; 36: e58. https://doi.org/10.3802/jgo.2025.36.e58.

[8] Raffone A, Raimondo D, Neola D, Travaglino A, Doglioli M, Ambrosio M, *et al*. Prevalence of sonographic signs in women with uterine sarcoma: a systematic review and meta-analysis. Ultraschall in Der Medizin (Stuttgart, Germany: 1980). 2024; 45: 293–304. https://doi.org/10.1055/a-2151-9205.

[9] Frijlingh M, Juffermans L, de Leeuw R, de Bruyn C, Timmerman D, van den Bosch T, *et al*. How to use power Doppler ultrasound in transvaginal assessment of uterine fibroids. Ultrasound in Obstetrics & Gynecology: the Official Journal of the International Society of Ultrasound in Obstetrics and Gynecology. 2022; 60: 277–283. https://doi.org/10.1002/uog.24879.

[10] Raffone A, Raimondo D, Neola D, Travaglino A, Raspollini A, Giorgi M, *et al*. Diagnostic Accuracy of Ultrasound in the Diagnosis of Uterine Leiomyomas and Sarcomas. Journal of Minimally Invasive Gynecology. 2024; 31: 28–36.e1. https://doi.org/10.1016/j.jmig.2023.09.013.

[11] Webber JT, Kaushik S, Bandyopadhyay S. Integration of Tumor Genomic Data with Cell Lines Using Multi-dimensional Network Modules Improves Cancer Pharmacogenomics. Cell Systems. 2018; 7: 526–536.e6. https://doi.org/10.1016/j.cels.2018.10.001.

[12] Wu J, Zhang H, Li L, Hu M, Chen L, Xu B, *et al*. A nomogram for predicting overall survival in patients with low-grade endometrial stromal sarcoma: A population-based analysis. Cancer Communications (London, England). 2020; 40: 301–312. https://doi.org/10.1002/cac2.12067.

[13] Bianchi L, Castellucci P, Farolfi A, Droghetti M, Artigas C,

Leite J, *et al*. Multicenter External Validation of a Nomogram for Predicting Positive Prostate-specific Membrane Antigen/Positron Emission Tomography Scan in Patients with Prostate Cancer Recurrence. European Urology Oncology. 2023; 6: 41–48. https://doi.org/10.1016/j.euo.2021.12.002.

[14] Gao SJ, Jin L, Meadows HW, Shafman TD, Gross CP, Yu JB, *et al*. Prediction of Distant Metastases After Stereotactic Body Radiation Therapy for Early Stage NSCLC: Development and External Validation of a Multi-Institutional Model. Journal of Thoracic Oncology: Official Publication of the International Association for the Study of Lung Cancer. 2023; 18: 339–349. https://doi.org/10.1016/j.jtho.2022.11.007.

[15] McCluggage WG, Singh N, Gilks CB. Key changes to the World Health Organization (WHO) classification of female genital tumours introduced in the 5th edition (2020). Histopathology. 2022; 80: 762–778. https://doi.org/10.1111/his.14609.

[16] Heremans R, Van Den Bosch T, Valentin L, Wynants L, Pascual MA, Fruscio R, *et al*. Ultrasound features of endometrial pathology in women without abnormal uterine bleeding: results from the International Endometrial Tumor Analysis study (IETA3). Ultrasound in Obstetrics & Gynecology: the Official Journal of the International Society of Ultrasound in Obstetrics and Gynecology. 2022; 60: 243–255. https://doi.org/10.1002/uog.24910.

[17] Wang Q, Lin Z, Zhu X, Wang Y, Zhang Y, He M, *et al*. Risk assessment and prediction of occult uterine sarcoma in patients with presumed uterine fibroids before high-intensity focused ultrasound treatment. International Journal of Hyperthermia: the Official Journal of European Society for Hyperthermic Oncology, North American Hyperthermia Group. 2024; 41: 2385600. https://doi.org/10.1080/02656736.2024.2385600.

[18] Chen X, Guo Q, Chen X, Zheng W, Kang Y, Cao D. Clinical and multiparametric MRI features for differentiating uterine carcinosarcoma from endometrioid adenocarcinoma. BMC Medical Imaging. 2024; 24: 48. https://doi.org/10.1186/s12880-024-01225-4.

[19] Kumagai K, Yagi T, Yamazaki M, Tasaki A, Asatani M, Ishikawa H. Quantitative MR texture analysis for the differentiation of uterine smooth muscle tumors with high signal intensity on T2-weighted imaging. Medicine. 2023; 102: e34452. https://doi.org/10.1097/MD.0000000000034452.

[20] Van Den Bosch T, Verbakel JY, Valentin L, Wynants L, De Cock B, Pascual MA, *et al*. Typical ultrasound features of various endometrial pathologies described using International Endometrial Tumor Analysis (IETA) terminology in women with abnormal uterine bleeding. Ultrasound in Obstetrics & Gynecology: the Official Journal of the International Society of Ultrasound in Obstetrics and Gynecology. 2021; 57: 164–172. https://doi.org/10.1002/uog.22109.

[21] Anneveldt KJ, van 't Oever HJ, Nijholt IM, Dijkstra JR, Hehenkamp WJ, Veersema S, *et al*. Systematic review of reproductive outcomes after High Intensity Focused Ultrasound treatment of uterine fibroids. European Journal of Radiology. 2021; 141: 109801. https://doi.org/10.1016/j.ejrad.2021.109801.

[22] Torkzaban M, Machado P, Gupta I, Hai Y, Forsberg F. Contrast-Enhanced Ultrasound for Monitoring Non-surgical Treatments of Uterine Fibroids: A Systematic Review. Ultrasound in Medicine & Biology. 2021; 47: 3–18. https://doi.org/10.1016/j.ultrasmedbio.2020.09.016.

[23] Yao F, Ding J, Lin F, Xu X, Jiang Q, Zhang L, *et al*. Nomogram based on ultrasound radiomics score and clinical variables for predicting histologic subtypes of epithelial ovarian cancer. The British Journal of Radiology. 2022; 95: 20211332. https://doi.org/10.1259/bjr.20211332.

[24] Suzuki A, Kido A, Matsuki M, Kotani Y, Murakami K, Yamanishi Y, *et al*. Development of an Algorithm to Differentiate Uterine Sarcoma from Fibroids Using MRI and LDH Levels. Diagnostics (Basel, Switzerland). 2023; 13: 1404. https://doi.org/10.3390/diagnostics13081404.

[25] WenTao J, GuoFu Z, TianPin W, ShiJia W, HaiYan Z, WenTao L. Nomogram for predicting the long-term outcomes of uterine artery embolization for adenomyosis. European Journal of Radiology. 2022; 148: 110183. https://doi.org/10.1016/j.ejrad.2022.110183.

[26] Taliento C, De Bruyn C, Ceusters J, Timmerman D, Van den Bosch T, Coosemans A. Circulating biomarkers for the preoperative diagnosis of uterine sarcoma: A systematic review and meta-analysis. Maturitas. 2025; 199: 108634. https://doi.org/10.1016/j.maturitas.2025.108634.